Biochemical Pharmacology, Vol. 54, pp. 657–668, 1997.

ISSN 0006-2952/97/$17.00 + 0.00
PII S0006-2952(97)00190-1

Pharmacokinetics, Metabolism, and Elimination of a 20-mer Phosphorothioate Oligodeoxynucleotide (CGP 69846A) after Intravenous and Subcutaneous Administration

J. A. Phillips, S. J. Craig,* D. Bayley,* R. A. Christian,* R. Geary† and P. L. Nicklin*‡*

*Novartis Horsham Research Centre, Horsham, West Sussex, RH12 4AB, UK, †Isis Pharmaceuticals, Inc., 2292 Faraday Ave, Carlsbad, CA 92008, USA

ABSTRACT. The pharmacokinetics, tissue distribution and metabolism of CGP 69846A, a 20-mer phosphorothioate oligodeoxynucleotide targeted against the 3′-untranslated region of human *c-raf*-1 kinase mRNA, were investigated *in vivo* in rats after intravenous and subcutaneous administration. Intravenous disposition studies with [^{3}H]CGP 69846A were supported with analysis by capillary gel electrophoresis and electrospray mass spectrometry. In combination, these techniques provide a detailed account of the pharmacokinetic and metabolic profile for this compound. The elimination of CGP 69846A after a single intravenous dose was studied over extended periods in mice using whole-body autoradiography and capillary gel electrophoresis. Subcutaneous administration to rats resulted in a significant bioavailability with peak plasma levels 4.5-fold lower than after intravenous dosing. This dose route resulted in low interanimal variability and only slightly greater metabolism of the oligonucleotide compared to the intravenous administration. BIOCHEM PHARMACOL **54**;6:657–668, 1997.

KEY WORDS. Antisense; c-*raf* kinase; ISIS 5132; oligonucleotide

The ability of antisense oligonucleotides (ODNs)§ to hybridise with target mRNA and cause protein-specific translation arrest [1, 2] has stimulated interest in their therapeutic potential [3], notably for tumour [4–6] and viral [7] indications. CGP 69846A, a 20-mer phosphorothioate oligonucleotide complementary to the 3′-untranslated region of human c-*raf*-1 kinase, can specifically knock-down c-*raf*-1 *in vitro* (IC_{50} between 50 and 100 nM) and has potent *in vivo* antitumour activity in the human tumour xenograft nude mouse model (at doses as low as 0.006 mg/kg) [5]. It is currently undergoing clinical evaluation.

The disposition of phosphorothioate oligonucleotides after intravenous [8–16], intradermal [9, 17], intraperitoneal [8–10, 18], and subcutaneous [9, 13] administration has been reported previously. In these studies, the metabolic status of the oligonucleotides was assessed using analytical methods lacking the precision (e.g. polyacrylamide slab gel electrophoresis) or specificity (e.g. high-performance liquid chromatography) for meaningful quantitation. Extraction methods and sensitive, high-resolution capillary electrophoretic assays have recently been developed that allow the parent oligonucleotide and its metabolites to be quantified in plasma, urine, and tissue samples [19]. In this study, these methods have been employed to support pharmacokinetic studies with [^{3}H]CGP 69846A after intravenous and subcutaneous administration to rats.

MATERIALS AND METHODS

Oligonucleotides

CGP 69846A (TsCsCsCsGsCsCsTsGsTsGsAsCsAsTsGs CsAsTsT where s = phosphorothioate; Lot number NGMP-0746-5132; otherwise known as ISIS 5132), was provided by Dr. Brett Monia of ISIS Pharmaceuticals (Carlsbad, CA); the active substance constitued a single peak by capillary gel electrophoresis and the molecular weight by electrospray mass spectrometry (6343.7 ± 1.3 Da) was consistent with the calculated value for this phosphorothioate

‡ Corresponding author: P. L. Nicklin, Novartis Horsham Research Center, Horsham, West Sussex, RH12 4AB, UK. TEL.: +44 1403 272827, FAX: +44 1403 323253, e-mail: paul.nicklin@pharma.novartis.com.

§ *Abbreviations:* AUC = area under the curve, Cl = clearance, C_{max} = maximum concentration, Da = Dalton, EDTA = ethylenediaminetetraacetic acid, HEPES = *N*-2-hydroxyethylpiperazine-*N*′-2-ethanesulphonic acid, μg equiv/g = microgram equivalents per gram of tissue, μg equiv/mL = microgram equivalents per millilitre of blood, mRNA = messenger ribonucleic acid, *m/z* = mass-to-charge ratio, N = parent oligonucleotide peak in capillary gel electrophoresis, N_{-n} = peaks migrating more rapidly than N in capillary gel electrophoresis, N_{+x} = peaks migrating more slowly than N in capillary gel electrophoresis, ODN = oligodeoxynucleotide, PS = phosphorothioate, RP-SPE = reverse-phase solid-phase extraction, SAX-SPE = strong anion-exchange solid-phase extraction, $t_{1/2\alpha}$ = half-life for distribution, $t_{1/2\beta}$ = half-life for elimination, T_{max} = time after dosing to maximum concentration, Tris = tris(hydroxymethyl)methylamine and V_d = volume of distribution.

Received 5 November 1996; accepted 27 March 1997.

sequence (6344.6 Da). [^{35}S]CGP 69846A was synthesised by Dr. Henri Sasmor of ISIS Pharmaceuticals. Poly-T_{27} phosphorothioate oligonucleotide, used as an internal standard for capillary gel electrophoretic analysis, was provided by ISIS Pharmaceuticals.

Animals

Male Wistar rats (240–270 g) and female Balb/c nu:nu nude mice (20 g) were fed *ad lib* with a standard laboratory diet (animals and husbandry supplies purchased from Bantin and Kingman, Hull, UK) and kept under controlled conditions (12-hr light cycle; 20°C). During experiments, the rats were housed in metabolism cages (North Kent Plastics, UK) with free access to food and water for up to 1440 min throughout the sampling period. The mice were housed in filter-top cages within a filtered positive pressure cabinet (Techniplast, Italy) and handled aseptically.

[^{3}H]Labelling of CGP 69846A

CGP 69846A was tritiated using the method described by Graham *et al.* [20] to produce 5′-TsCsCsCs[3H]GsCsCsTs[3H]GsTs[3H]Gs[3H]AsCs[3H]AsTs[3H]GsCs[3H]AsTsT-3′. The reaction product was shown to have a radiochemical purity greater than 97% and a specific activity of 324 Ci/mol. [^{3}H]CGP 69846A was thermally stable below 95°C in line with a specific tritiation at the C8-position of purine bases (data not shown).

Intravenous Administration Studies to Rats

Animals were immobilised through light sedation induced by a 100 μL, 0.13 mg/mL intramuscular injection of fentanyl citrate (Hypnorm, Janssen Pharmaceuticals Ltd., Oxford, UK). [^{3}H]CGP 69846A, 0.5 μCi in 100 μL 0.9% saline at doses of 0.06, 0.6, 6.0, or 60 mg/kg, was administered intravenously by tail vein injection. Aliquots of blood (200 μL) were withdrawn from the contralateral tail vein 5, 15, 30, 60, 120, 240, 360, and 1440 min after dosing. Animals were killed by sodium pentabarbitone overdose (Expiral, Sanofi Animal Welfare, UK) after 10, 360, or 1440 min. Tissues of interest (blood, urine, liver, kidney, spleen, heart, lung, thymus, pancreas, adrenals, mesenteric lymph nodes, salivary glands, testes, muscle, skin, bone, fat, eye, brain, duodenum, ileum, and colon) were immediately collected and their [^{3}H]-content determined. Identical experiments were performed, at a dose of 6.0 mg/kg with sacrifice at 10, 120, 360, and 1440 min, for tissue analysis by capillary gel electrophoresis.

Subcutaneous Administration Studies to Rats

Animals were immobilised through light sedation induced by a 100 μL, 0.13 mg/mL intramuscular injection of fentanyl citrate (Hypnorm, Janssen Pharmaceuticals Ltd., Oxford, UK). [^{3}H]CGP 69846A, 0.5 μCi in 100 μL 0.9% saline at doses of 0.6, 6.0, or 60 mg/kg, was administered subcutaneously by injection into the scruff of the neck. Aliquots of blood (200 μL) were withdrawn from the tail vein 5, 15, 30, 60, 120, 240, 360, and 1440 min after dosing. At the end of the experiment, animals were killed by sodium pentabarbitone overdose (Expiral, Sanofi Animal Welfare, UK). Tissues of interest (blood, urine, feces, liver, kidney, spleen, heart, lung, thymus, pancreas, adrenals, mesenteric lymph nodes, salivary glands, testes, muscle, skin, bone, fat, eye, brain, duodenum, ileum, colon, and injection site) were immediately collected and their [^{3}H]-content determined. Identical experiments were performed, at a dose of 6.0 mg/kg with sacrifice at 360 min and 1440 min, for tissue analysis by capillary gel electrophoresis.

[^{3}H]-Quantitation

The [^{3}H]-content of blood, urine, and preweighed tissue samples was determined using a tissue-oxidiser (Canberra-Packard 306) followed by liquid scintillation counting (Beckman LS6500). The oxidizer efficiency ranged from 90 to 96%. The [^{3}H]-content of each sample was adjusted for total tissue weight and expressed as a percentage of the dose administered or as the equivalent concentration of CGP 69846A (μg equiv/mL or μg equiv/g). For calculations of tissue content, muscle, skin, bone, and fat were assumed to be 41, 16, 10, and 10% of total body weight, respectively.

Elimination Studies in Mice

WHOLEBODY AUTORADIOGRAPHY STUDIES. Twelve nude mice were divided into four groups that experienced different dose regimens. [^{35}S]CGP 69846A (total radiochemical dose of 1 μCi) was administered intravenously to each animal according to the schedule given in Table 1. Animals were killed by asphyxiation with carbon dioxide, 60 min after receiving the last dose. Each was pinned to a cork board to ensure retention of a consistent shape during freezing by total immersion in hexane cooled to −76°C with solid carbon dioxide. Frozen cadavers were subsequently embedded in cold carboxymethyl cellulose. The frozen blocks were sectioned on a PMV wholebody cryostat at −15 to −20°C. Six 20 μM sections were cut at each of six levels, mounted onto 3M adhesive tape and freeze dried. Freeze-dried sections were applied to tritium-film (Amersham International, UK) and exposed for 4 weeks at −20°C. After the exposure period, the film was developed in Kodak D19 developer at 20°C for 4 min, rinsed with water, fixed in 20% aqueous thiosulphate for 5 min, washed for 30 min with running water, and air dried.

CAPILLARY GEL ELECTROPHORETIC STUDIES. Nude mice were dosed intravenously with a single dose of CGP 69846A at 6.0 mg/kg by tail vein injection. At 1, 3, 7, and 10 days after dosing, groups of three animals were killed by cervical dislocation. Animals were exsanguinated by cardiac puncture. Plasma, kidney, and liver were frozen

TABLE 1. Dosing regimen for whole-body autoradiography elimination studies

Day	Group 1 (single 10 mg/kg dose)	Group 2 (single 10 mg/kg dose)	Group 3 (daily 10 mg/kg doses)	Group 4 (daily 10 mg/kg doses)
1	saline	[^{35}S]CGP69846A(1.00μCi)	[^{35}S]CGP69846A(0.143μCi)	CGP 69846A
2	saline	saline	[^{35}S]CGP69846A(0.143μCi)	CGP 69846A
3	saline	saline	[^{35}S]CGP69846A(0.143μCi)	CGP 69846A
4	saline	saline	[^{35}S]CGP69846A(0.143μCi)	CGP 69846A
5	saline	saline	[^{35}S]CGP69846A(0.143μCi)	CGP 69846A
6	saline	saline	[^{35}S]CGP69846A(0.143μCi)	CGP 69846A
7	[^{35}S]CGP 69846A (1.00 μCi)	saline	[^{35}S]CGP69846A(0.143μCi)	[^{35}S]CGP 69846A (1.00 μCi)

Groups represent the following; 1 = single dose whole-body distribution, 2 = single dose whole-body distribution after 7 days of elimination, 3 = repeated dose whole-body distribution, 4 = single dose [^{35}S]CGP 69846A whole-body distribution following repeated CGP 69846A administration. The total radioactive dose was 1 μCi in all cases.

(−20°C) prior to analysis by capillary gel electrophoresis (see below).

Extraction and Analysis of Plasma and Tissue Samples

EXTRACTION. Plasma samples were extracted as described by Leeds *et al.* [19]. Tissue samples (150 mg) were homogenized in Tris buffer pH 8.0 (20 mM Tris-HCl, 20 mM EDTA, 0.1 M NaCl, 0.5% NP 40) containing 200 nM of poly-T_{27} as an internal standard. The homogenate was incubated overnight at 37°C together with proteinase K (final concentration 1.5 mg/mL; Boehringer, UK) and extracted twice with phenol/chloroform (volume ratio 2:1). The aqueous phases were concentrated using a vacuum drier (MAXI dry plus, Heto, Denmark), treated overnight with 50 μL of 30% ammonium hydroxide at 55°C and concentrated once again. The samples were loaded onto a pre-equilibrated strong anion-exchange solid-phase extraction cartridge (SAX-SPE; Accubond 100 mg, J+W Scientific, USA) in loading-buffer (5.0 mL; 10 mM Tris-HCl, pH 9.0, 0.5 M KCl, 20% acetonitrile), washed with 3.0 mL of loading buffer, and eluted with 3.0 mL elution-buffer (10 mM Tris-HCl, pH 9.0, 0.5 M KCl, 1.0 M NaBr, 30% acetonitrile). The SAX-SPE eluate was loaded onto a preequilibrated RP-SPE cartridge (C_{18} end-capped Isolute 100 mg; International Sorbent Technology, USA), washed with 5.0 mL of Nanopure water, and eluted with 4.0 mL of 20% aqueous acetonitrile. The RP-SPE eluate was concentrated using a vacuum drier and reconstituted to 30 μL with Nanopure water. The sample was further desalted by placing it on a 0.025 μm membrane filter (VS Millipore, UK) floating on Nanopure water for 60 min. Analyses were performed by capillary gel electrophoresis.

CAPILLARY GEL ELECTROPHORESIS. Plasma and tissue samples were analysed by capillary gel electrophoresis (Beckman P/ACE 5010, Beckman, UK) using a 20 cm (effective length) 10 or 12% polyacrylamide gel at 30°C with an applied voltage of 550 V/cm. Oligonucleotides were detected at 260 nm. Under these conditions, baseline resolution of CGP 69846A from its chain-shortened metabolites was achieved. Oligonucleotide and metabolite concentrations were normalised for recovery and variability by comparison with the T_{27} internal standard using Eqn. 1.

$$C_2 = C_1(E_1/E_2)[(A_2/T_{m2})/(A_1/T_{m1})] \quad (1)$$

where; C_1 = concentration of the standard, C_2 = concentration of the sample, E_1 = molar extinction coefficient of the standard, E_2 = molar extinction coefficient of the sample, A_1 = area of the standard peak, A_2 = area of the sample peak, T_{m1} = migration time of the standard peak and T_{m2} = migration time of the sample peak.

The limit of detection was approximately 0.07 μg/mL in plasma and approximately 0.1 μg/g in tissue. Labelling of the oligonucleotide components in plasma and tissue extracts using [γ^{32}P]-ATP and T4-polynucleotide kinase, followed by separation and visualisation on a 20% sequencing gel, did not reveal any band not detected by capillary gel electrophoresis (data not shown).

MASS SPECTROMETRY. Liver tissue extracts were analysed by mass spectrometry using a Micromass Platform II (Altrincham, UK), having an m/z range of 3000, equipped with an electrospray interface. Samples were analysed in negative ion-mode by directly injecting 10 μL into the electrospray source via a loop injector after a 50% dilution with acetonitrile:water (1:1) containing 2% tripropylamine. The electrospray mobile phase was acetonitrile:water (1:1) at a flow rate of 10 μL/min, using a Gilson 305 pump. The mass spectrometer was scanned over an m/z range of 400 to 1200 and source conditions were optimised for each sample; typical values were capillary potential 2.31 kV, counter electrode 0.43 kV, and cone voltage 41 V. The source was maintained at a temperature of 60°C, with a drying gas flow of 200 L/hr and a nebulising gas flow of 15–20 L/hr.

RESULTS

Blood Kinetics of [^{3}H]CGP 69846A after Intravenous Administration

Intravenous administration of 0.6 mg/kg [^{3}H]CGP 69846A resulted in a biphasic profile for the disappearance of radiolabel from blood (Fig. 1A). A rapid distribution-phase (0–240 min; $t_{1/2\alpha}$ = 19 min) was followed by a prolonged elimination phase (240 min onwards; $t_{1/2\beta}$ = 775 min) during which circulating tritium levels were less than 1.0% of the administered dose. The total blood clearance (Cl) was 2.33 mL/min/kg. The volume of distribution (V_d) of

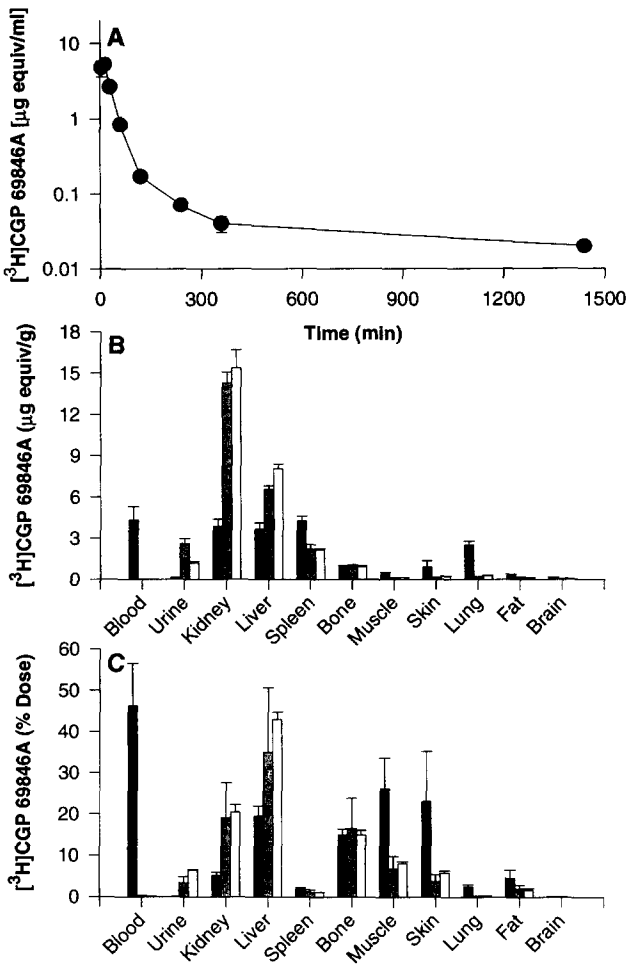

FIG. 1. Blood kinetics (A) and tissue distribution (B,C) of [^{3}H]CGP 69846A (0.6 mg/kg) following intravenous administration to rats. (B, C) Black bars = 10 min, gray bars = 360 min, and white bars = 1440 min. Mean ± SEM, n = 4.

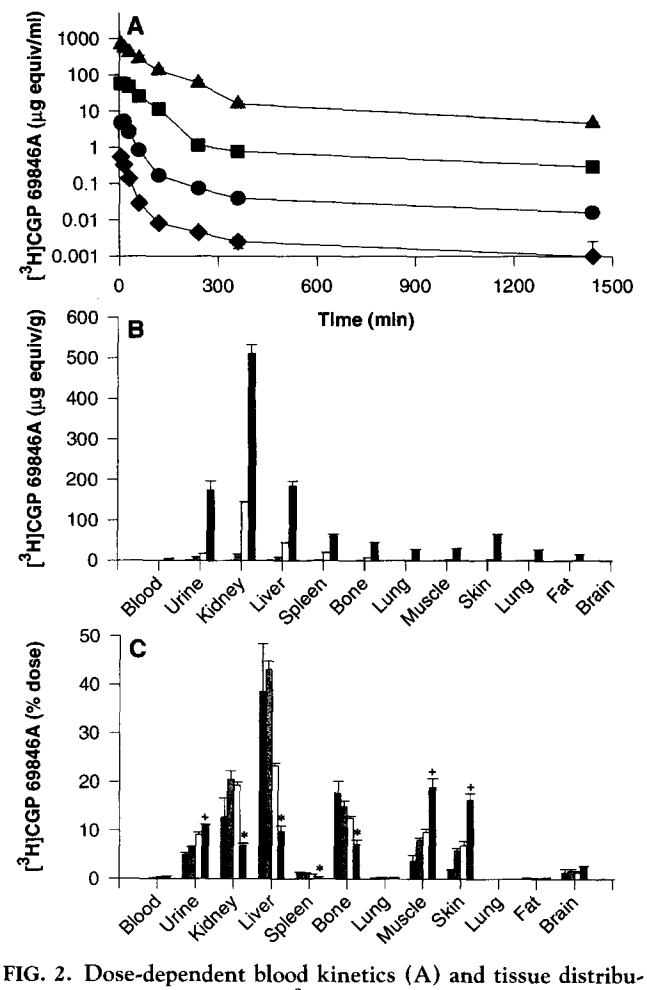

FIG. 2. Dose-dependent blood kinetics (A) and tissue distribution at 1440 min (B,C) of [^{3}H]CGP 69846A following intravenous administration to rats. (A) Diamonds = 0.06 mg/kg, circles = 0.6 mg/kg, squares = 6.0 mg/kg, and triangles = 60.0 mg/kg. (B, C) Black bars = 0.06 mg/kg, light gray bars = 0.6 mg/kg, white bars = 6.0 mg/kg, and dark gray bars = 60.0 mg/kg. Mean ± SEM for n = 3–6, * Denotes significantly lower and + denotes significantly higher ($P < 0.05$) at 60.0 mg/kg compared to 0.06 mg/kg.

651 mL (or 2602 mL/kg) was approximately fivefold greater than the total body water volume of the rat.

The blood kinetics of intravenously administered [^{3}H]CGP 69846A were dose dependent in rats (Fig. 2A). The half-life of the distribution-phase ($t_{1/2\alpha}$) increased as the dose increased in a stepwise manner; 0.06 mg/kg = 12 min, 0.6 mg/kg = 19 min, 6.0 mg/kg = 40.5 min, and 60 mg/kg = 48 min. The percentage of administered dose remaining in the blood after 360 min was 0.28 ± 0.20, 0.42 ± 0.20, 0.83 ± 0.06, and 1.70 ± 0.58%, for the animals in the 0.06, 0.6, 6.0, and 60 mg/kg groups, respectively.

Capillary Gel Electrophoretic Analysis of Plasma Samples

CGP 69846A was detectable by capillary gel electrophoresis in plasma at 10, 120, and 360, but not 1440 min (Fig. 3A to D; Table 2). Intact CGP 69846A represented 60.9, 48.3, and 18.1% of the total peak area at 10, 120, and 360 min, respectively. In addition to the parent molecule (N), chain-shortened metabolites (N_{-n} nucleotides) were observed to migrate more rapidly than the parent compound. At 10 and 120 min, N_{-1}, N_{-2}, and N_{-3} species were the major metabolites (≥5% of the total oligonucleotide pool). At 360 min, low circulating levels of CGP 69846A and its major metabolites, namely N_{-1}, N_{-2}, N_{-3}, N_{-4}, N_{-8}, and N_{-9}, were detected. N_{-6} was a minor metabolite whilst N_{-5} and N_{-7} were not detected.

Tissue Distribution of [^{3}H]CGP 69846A after Intravenous Administration

Rats were killed at 10, 360, or 1440 min following intravenous administration of 0.6 mg/kg [^{3}H]CGP 69846A and a distinctive tissue distribution was observed (Fig. 1B and C). The liver was the major organ of distribution, accounting for 43.0 ± 1.8% of the 0.6 mg/kg intravenous dose after 1440 min and attaining a concentration of 8.05 ± 0.16 μg

TABLE 2. Capillary gel electrophoretic analysis of CGP 69846A and its metabolites in plasma, kidney, and liver following intravenous administration of rats

Time (min)	Concentration (μg/g)									
	N	N_{-1}	N_{-2}	N_{-3}	N_{-4}	N_{-5}	N_{-6}	N_{-7}	N_{-8}	N_{-9}
Plasma										
10	36.9 ± 3.1	12 ± 0.9	5.3 ± 0.4	2.8 ± 0.2	1.0 ± 0.1	0.4 ± 0.02	0.12	0.01	n.d.	n.d.
120	6.1 ± 1.6	2.8 ± 0.1	1.5 ± 0.03	0.9 ± 0.1	0.5 ± 0.1	0.2 ± 0.1	0.1 ± 0.1	0.3 ± 0.1	0.3 ± 0.1	0.1 ± 0.04
360	0.1 ± 0.02	0.1 ± 0.01	0.1 ± 0.01	0.03 ± 0.01	0.03 ± 0.01	n.d.	0.02 ± 0.02	n.d.	0.1 ± 0.03	0.2 ± 0.06
1440	n.d.	n.d.	n.d.	n.d.	n.d.	n.d.	n.d.	n.d.	n.d.	n.d.
Kidney										
10	20.7 ± 0.6	10.1 ± 0.3	6.2 ± 0.3	4.2 ± 0.2	1.6 ± 0.4	1.2 ± 0.2	0.5 ± 0.1	n.d.	n.d.	n.d.
120	34.9 ± 11.0	25.2 ± 7.9	19.9 ± 5.8	13.8 ± 3.6	6.7 ± 1.3	4.4 ± 0.8	3.1 ± 0.7	1.3 ± 0.8	0.6 ± 0.5	0.6
360	49.2 ± 6.3	40.6 ± 5.3	34.4 ± 4.1	25.6 ± 2.6	15.3 ± 0.4	11.5 ± 0.2	9.6 ± 0.2	5.9 ± 0.4	5.6 ± 0.8	3.2 ± 0.9
1440	19.5 ± 2.3	15.9 ± 1.8	12.0 ± 1.2	8.2 ± 0.6	3.7 ± 0.1	2.5 ± 0.3	1.5 ± 0.4	0.8 ± 0.6	0.3 ± 0.2	n.d.
Liver										
10	19.0 ± 6.0	8.4 ± 2.3	3.5 ± 1.7	2.7 ± 1.2	1.0 ± 0.1	0.1 ± 0.1	0.05	n.d.	n.d.	n.d.
120	22.4 ± 1.3	12.8 ± 1.6	6.4 ± 1.9	3.1 ± 1.6	0.9 ± 0.5	0.9 ± 0.4	0.8 ± 0.6	0.5 ± 0.1	0.1 ± 0.01	n.d.
360	19.4 ± 1.1	12.7 ± 0.7	6.9 ± 0.7	3.6 ± 0.9	1.5 ± 0.6	0.7 ± 0.3	1.0 ± 0.4	0.5 ± 0.1	0.03 ± 0.02	n.d.
1440	11.8 ± 2.6	9.5 ± 1.9	6.1 ± 1.1	3.9 ± 0.8	3.7 ± 0.5	1.3 ± 0.2	1.8 ± 0.7	0.7 ± 0.3	0.2 ± 0.1	n.d.

Data represent mean ± SEM for three animals, where metabolites are not present on all three animals mean values are given without experimental errors. n.d. = not detected.

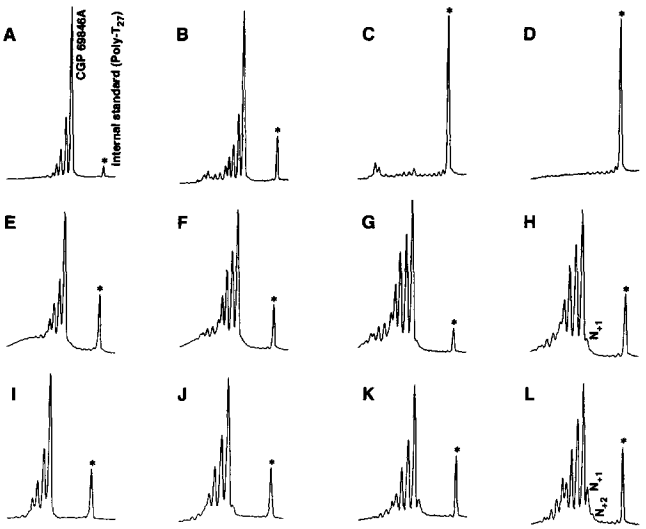

FIG. 3. Capillary gel electrophoresis of plasma, kidney, and liver extracts following intravenous administration of CGP 69846A (6.0 mg/kg) to rats. Plasma: A = 10 min, B = 120 min, C = 360 min, and D = 1440 min; Kidney: E = 10 min, F = 120 min, G = 360 min, and H = 1440 min; I = 10 min, J = 120 min, K = 360 min, and L = 1440 min. N_{+1} and N_{+2} represent slower-migrating metabolites and * denotes T_{27} internal standard.

equiv/g. The highest concentration was achieved in the kidney; 15.4 ± 0.7 μg equiv/g of [^{3}H]CGP 69846A after 1440 min, which represented 20.5 ± 1.8% of the total radioactive dose. Organs were categorised according to the relative tissue-to-blood (T:B) concentration ratios at 240 min after a 6.0 mg/kg dose (Table 3). High accumulating organs were kidney (T:B = 38.0), liver, spleen, mesenteric lymph nodes, salivary gland, duodenum, and adrenal gland. Low accumulating tissues (i.e. T:B <10% of the value for kidney, <3.80) were ileum, bone (intact femur), pancreas, colon, skin, lung, thymus, skeletal muscle, heart, eye, and testes. Negligible accumulating tissues (i.e. T:B <1% of the value for kidney, <0.38) were fat and brain. Although bone (intact femur) was defined as a low accumulating tissue according to these criteria, it behaved as a high accumulating tissue. Because greater than 85% of the bone-associated radioactivity was localised to the bone marrow (data not shown), the most likely explanation is that bone marrow was a high accumulating tissue but it represents a small fraction of the total bone mass.

The tissue distribution of [^{3}H]CGP 69846A was dose dependent (Fig. 2B and C). The percentage of radiolabel distributed to liver, kidney, bone, and spleen decreased with increasing dose. The concentration of radiolabeled oligonucleotide associated with tissue increased in a dose-related, but not dose-linear fashion. As the intravenous dose increased from 0.06 to 60 mg/kg, the proportion accumulating in the liver and kidney decreased from 38.5 ± 4.1% to 9.8 ± 1.2%, and from 20.5 ± 1.8% to 6.8 ± 0.5% at 1440 min, respectively. This was matched by a reduced clearance from blood and concomitant increase in the

TABLE 3. Tissue distribution of [^{3}H]CGP 69846A (6.0 mg/kg at 240 min) giving tissue:blood concentration ratios for tissues

Tissue	Amount (% dose)	Concentration (μg equiv/g)	Tissue:blood (concentration ratio)	Tissue type
Blood	2.61 ± 1.04	2.45 ± 0.40	1.0	—
Urine	5.16 ± 0.66	67.64 ± 4.31	27.6	—
Kidney	12.41 ± 0.64	93.08 ± 1.97	38.0	high
Liver	23.50 ± 0.44	44.06 ± 0.34	18.0	high
Spleen	0.98 ± 0.06	21.01 ± 0.33	8.6	high
Mesenteric lymph nodes	0.54 ± 0.22	16.34 ± 2.67	6.8	high
Salivary gland	0.39 ± 0.07	11.68 ± 0.82	4.8	high
Duodenum	0.65 ± 0.30	13.89 ± 2.66	5.7	high
Adrenal gland	0.05 ± 0.01	11.32 ± 0.65	4.6	high
Ileum	3.68 ± 0.42	7.08 ± 0.33	2.9	low
Bone	11.40 ± 0.60	6.84 ± 0.15	2.8	low
Pancreas	0.38 ± 0.03	5.74 ± 0.16	2.3	low
Colon	0.62 ± 0.24	3.11 ± 0.49	1.3	low
Skin	8.32 ± 0.76	3.20 ± 0.12	1.3	low
Lung	0.28 ± 0.01	2.82 ± 0.08	1.2	low
Thymus	0.07 ± 0.01	2.48 ± 0.10	1.0	low
Skeletal muscle	15.52 ± 2.97	2.33 ± 0.18	0.9	low
Heart	0.12 ± 0.01	2.31 ± 0.06	0.9	low
Eye	0.02 ± 0.001	1.39 ± 0.02	0.6	low
Gonads	0.20 ± 0.03	1.18 ± 0.07	0.5	low
Fat	0.78 ± 0.52	0.47 ± 0.13	0.2	negligible
Brain	0.01 ± 0.01	0.12 ± 0.02	0.05	negligible

association with well-perfused low-affinity tissues. Skeletal muscle-associated [^{3}H]CGP 69846A, for instance, increased from 3.6 ± 0.5% at 0.06 mg/kg to 18.9 ± 1.8% of the total radioactive dose at 60 mg/kg. The fecal and urinary excretion of was low [^{3}H]CGP 69846A over this dose range (data not shown).

Capillary Gel Electrophoretic Analysis of Tissue Samples

CGP 69846A was detectable by capillary gel electrophoresis in the kidney and liver at all time points (Fig. 3E to L; Table 2). In the kidney, intact CGP 69846A represented 43.8, 28.0, 21.1, and 27.2% at 10, 120, 360, and 1440 min, respectively. Intact compound in the liver represented 53.3, 46.3, 38.1, and 24.4% at the same time points. In addition to the parent molecule (N), chain-shortened metabolites (N_{-n} nucleotides) were observed; N_{-1} to N_{-5} represented the major metabolites (≥5% of the oligonucleotide pool) while N_{-6} to N_{-9} represented the minor metabolites. The concentration–time profile for intact CGP 69846A in plasma, kidney, and liver are shown by Fig. 4A; similar profiles for CGP 69846A and its major metabolites in the kidney and liver are given in Fig. 4B and C, respectively. CGP 69846A accumulated in the kidney, achieving its maximal concentration (C_{max}) of 49.2 ± 6.3 μg/g after 360 min before decreasing to 19.5 ± 2.3 μg/g at 1440 min. The concentration–time profiles of the major metabolites paralleled that for the parent compound. In the liver, CGP 69846A accumulated to its C_{max} of 22.4 ± 1.3 μg/g by 120 min before decreasing to 11.8 ± 2.6 μg/g at 1440 min. For this organ, the concentration–time profiles for the major metabolites did not mirror that of the parent compound. The time to achieve C_{max} increased across the metabolites series N_{-1} to N_{-5}, ultimately resulting in a net accumulation of the higher order metabolites over the duration of these experiments.

Peaks that migrated more slowly than CGP 69846A (denoted N_{+x}; Fig. 3H and L) were also observed in extracts from kidney and liver. These species increased with time. In the kidney an N_{+1} peak (1.8 ± 0.9% of the oligonucleotide pool) was observed whereas N_{+1} and N_{+2} species were detected in the liver and accounted for 6.5 ± 0.5% and 1.5 ± 0.4% of the total oligonucleotide pool at 1440 min, respectively.

Electrospray Mass Spectroscopic Analysis of Liver Samples

A typical electrospray spectrum for a 1440 min liver sample showed CGP 69846A and a series of chain-shortened metabolites differing in mass by approximately one nucleotide unit; this profile agreed with capillary gel electrophoretic analysis in terms of peak numbers and their relative abundance (Fig. 5). These peak clusters were composed of multiple species apparently unresolved by capillary gel electrophoresis. Components having masses consistent with progressive loss of nucleotides from the 3′-end alone, the 5′-end alone and from both ends were identified (Table 4). Evidence for more subtle metabolism, corresponding to the additional loss of 16 Da from CGP 69846A and its metabolites, was also observed. Finally, a metabolite with greater mass (+382 Da) than the parent compound was detected but not identified. All metabolites

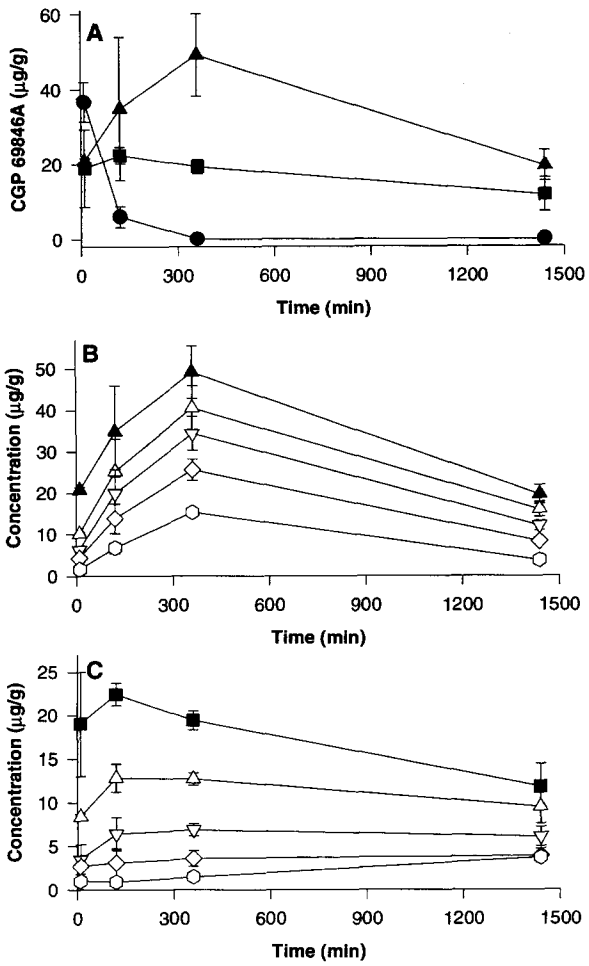

FIG. 4. Concentration–time profiles for (A) CGP 69846A in plasma, kidney, and liver, (B) CGP 69846A and its major metabolites in kidney, and (C) CGP 69846A and its major metabolites in liver after intravenous administration. (A) circles = plasma, triangles = kidney and squares = liver. (B) (kidney): solid triangles = N, open triangles = N_{-1}, open inverted triangles = N_{-2}, open diamond = N_{-3} and open hexagon = N_{-4}. (C) (liver): solid squares = N, open triangles = N_{-1}, open inverted triangles = N_{-2}, open diamond = N_{-3}, and open hexagon = N_{-4}. Mean ± SEM, n = 3.

resulted from *in vivo* biotransformation because the extraction procedure was without effect on CGP 69846A and control liver extracts did not produce interfering signals (data not shown).

Blood Kinetics of [^{3}H]CGP 69846A after Subcutaneous Administration

Subcutaneous administration of [^{3}H]CGP 69846A to rats, resulted in significant blood concentrations (Fig. 6A). As the dose increased from 0.6 to 6.0 to 60.0 mg/kg, both the C_{max} (0.37 ± 0.14, 12.8 ± 1.20, and 154 ± 4.11 µg equiv/ml, respectively) and T_{max} (30, 60, and 120 min, respectively) increased. Calculated from comparative intravenous AUCs, the bioavailability of this route increased from 41 to ≈100% as the dose increased from 0.6 mg/kg to

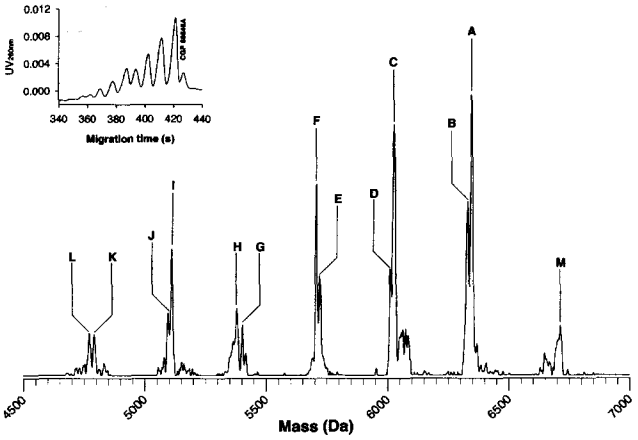

FIG. 5. Electrospray mass spectrum of CGP 69846A and its metabolites extracted from rat liver. Capillary gel electrophoerogram for the liver extract is shown as the insert. Peak assignment is detailed in Table 4.

60 mg/kg (Table 5). The total radioactivity recovered in tissues at 1440 min showed a similar trend.

Tissue Distribution of [^{3}H]CGP 69846A after Subcutaneous Administration

Tissue distribution pattern for [^{3}H]CGP 69846A after subcutaneous administration was similar to that for intravenous administration (Fig. 6B,C). The liver-associated radioactivity accounted for the largest proportion of dose while the kidney exhibited the highest radiolabel concentration. The distribution to tissues was dose dependent, but not dose linear, over the dose range studied (0.6 to 60 mg/kg). The metabolism of intravenously and subcutaneously administered CGP 69846A were compared (Table 6). Parent oligonucleotide or metabolites were not detected in plasma at 360 min or 1440 min. The metabolite profile in kidney and liver extracts provided evidence for slightly greater metabolism following subcutaneous administration compared with the same dose given intravenously.

Elimination Kinetics from Mice

The elimination of CGP 69846A from organs over prolonged periods was investigated in nude mice using two methods, (i) whole-body autoradiography, and (ii) analysis of kidney and liver extracts by capillary gel electrophoresis between 1 and 10 days after a single dose. The tissue distribution of CGP 69846A in mice is similar to that in rats, one notable distinction being that a greater proportion of the dose was associated with the skin of mice (data not shown). One day after dosing, the whole body distribution for [^{35}S]CGP 69846A was comparable to the tissue distribution of [^{3}H]CGP 69846A by radiochemical quantitation studies; it accumulated within the kidney cortex, liver, and spleen, was diffusely associated with low accumulating tissues and did not penetrate into the central nervous system or eyes (Fig. 7, group 1). Seven days after dosing,

TABLE 4. Assignment of mass peaks corresponding to CGP 69846A metabolites in liver

Peak	M_r measured	Possible metabolites	3′-loss	5′-loss	Other	M_r calculated
A	6343.7 ± 1.3	(i)				6344.6
B	6329.0 ± 2.4	(i)			−16 Da	6328.6
C	6024.4 ± 0.8	(i)	T			6023.6
		(ii)		T		6023.6
D	6007.8 ± 0.4	(i)	T		−16 Da	6007.6
		(ii)		T	−16 Da	6007.6
E	5719.4 ± 0.8	(i)		TC		5718.5
F	5702.8 ± 1.5	(i)	TT			5703.5
		(ii)		TC	−16 Da	5702.5
		(iii)	T	T		5702.5
G	5409.9 ± 0.4	(i)		TCC		5413.5
H	5375.8 ± 3.5	(i)	ATT			5374.5
I	5109.3 ± 1.5	(i)		TCCC		5108.5
J	5092.8 ± 0.4	(i)	T	TCC		5092.5
		(ii)		TCCC	−16 Da	5092.5
K	4786.3 ± 2.0	(i)	TT	TCC		4787.4
		(ii)	T	TCCC		4787.4
L	4771.3 ± 1.7	(i)	TT	TCC	−16 Da	4771.4
			T	TCCC	−16 Da	4771.4
M	6725.4 ± 0.4	(i)			+382 Da	n.a.

n.a. = not assigned.

tissue-associated radioactivity was much reduced with low levels still present in the kidney cortex and trace levels being associated with the liver (Fig. 7, group 2). These elimination kinetics were confirmed by the analysis of kidney and liver samples by capillary gel electrophoresis (Fig. 8).

DISCUSSION

This study reports the pharmacokinetics, tissue distribution, and metabolism of a 20-mer phosphorothioate oligonucleotide after intravenous and subcutaneous administration. Radiochemical studies were supported by extensive analysis of plasma and tissue samples by capillary gel electrophoresis. Moreover, metabolites accumulating in the liver were characterised by electrospray mass spectrometry.

The blood kinetics of intravenously administered [^{3}H]CGP 69846A were biphasic; an initial rapid clearance was followed by a prolonged circulation of radiolabel. Although CGP 69846A was metabolised during the initial phase (see below), its distribution to tissues was the primary mechanism for clearance from the blood compartment. Indeed, [^{3}H]CGP 69846A was rapidly distributed amongst high (e.g. kidney, liver, spleen), low (e.g. lung, skeletal muscle, skin), and negligible (e.g. brain, fat) accumulating tissues. In the rat, the principle accumulating organs were the kidney and liver; the highest concentration was achieved in the kidney, while the liver accounted for the greatest proportion of the dose by virtue of its greater tissue mass. This accumulation in specific tissues was reflected in a volume of distribution fivefold higher than the total body volume of the rat. Meaningful comparison of these observations with those reported for phosphorothioate oligonucleotides by other workers is difficult because of experimental variables (oligonucleotide length, dose, radiolabel, detection methods, and animal species) and sequence effects (J. Phillips, unpublished observations). Nevertheless, the disposition of [^{3}H]CGP 69846A was broadly similar to that of other phosphorothioate oligonucleotides reported in the literature [8–16]. To extend previous work, the influence of dose on the disposition of a phosphorothioate oligonucleotide has been investigated systematically. The distribution to high accumulating tissues was saturable and resulted in nonlinear pharmacokinetics. As the administered dose increased, the proportion distributed to the high accumulating tissues decreased significantly. At the same time, plasma clearance was reduced and distribution to well-perfused low accumulating tissues increased. These data are consistent with high accumulating tissues having saturable uptake mechanisms (e.g. receptor- mediated membrane transport) for CGP 69846A. The oligonucleotide would be less efficiently extracted from the blood upon saturation of renal and hepatic uptake. In turn, the prolonged circulation time could explain the increased association with well-perfused, low accumulating tissues. In our experience, nonlinear pharmacokinetics is especially prominent in rats and less so in other species such as mice. Further studies are required to establish whether similar nonlinearity occurs in monkeys and human subjects. Our previous work with another 20-mer phosphorothioate oligonucleotide (CGP 64128A, otherwise known as ISIS 3521) has shown that, in addition to a distinctive organ distribution, it was taken up by specific cell types within tissues *in vivo*; proximal tubular cells in the kidney and Kupffer or endothelial cells in the liver [21]. This dose-dependent and cell type specific uptake by high accumulating organs is analogous to the saturable

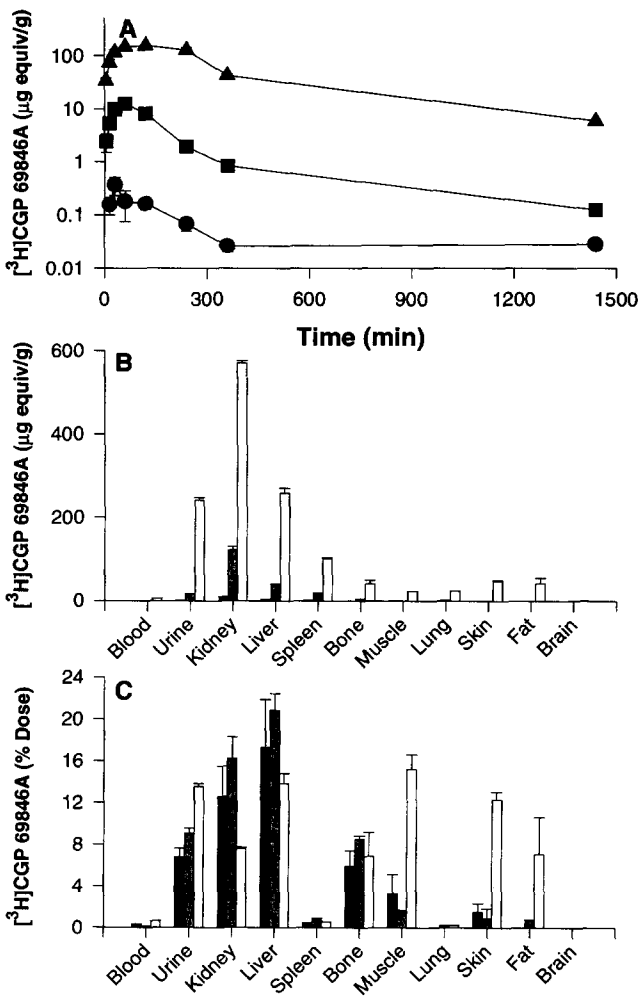

FIG. 6. Blood kinetics (A) and tissue distribution (B, C) of [^{3}H]CGP 69846A following subcutaneous administration to rats. (A) Circles = 0.6 mg/kg, squares = 6.0 mg/kg, and triangles = 60.0 mg/kg. (B, C) Black bars = 0.6 mg/kg, gray bars = 6.0 mg/kg, and white bars = 60.0 mg/kg. Mean ± SEM, n = 4.

and cell line-dependent uptake reported for phosphorothioate oligonucleotides *in vitro* [22, 23]. The nature of the cell type specific and saturable uptake into high affinity tissues *in vivo* is currently under investigation in our laboratories.

By analogy with other phosphorothioate oligonucleotides, partial metabolism of [^{3}H]CGP 69846A would be expected over the time-course of these experiments [8, 11, 15]. This could potentially liberate radiolabelled mononucleotides and complicate the interpretation of the disposition data. Radiochemical studies were, therefore, supported by the analysis of CGP 69846A and its metabolites in tissue extracts by capillary gel electrophoresis. A 6.0 mg/kg dose was selected since it is relevant to *in vivo* pharmacodynamic studies [5] and tissue concentrations were within the working range for the analytical methodology. Oligonucleotides were detected in the blood for up to 360 min post administration, circulating as CGP 69846A and a series of chain-shortened metabolites. The plasma half-life of intact CGP 69846A (≈30 min) was comparable to that of the radiolabeled compound (40.5 min) at the same 6.0 mg/kg dose. The rapid initial metabolism of the parent compound in plasma was followed by an apparent decrease in the rate of degradation (i.e. 39% loss of CGP 69846A within 10 min but only a 51.7% loss by 120 min). The reasons for this phenomenon are unclear, however, possible explanations include the inhibition of nucleases *in vivo* (which has previously been observed *in vitro* [3]) and/or the distribution of R_p and S_p phosphorothioate diastereoisomers, with their significantly different nuclease resistances [24], in the oligonucleotide. Nevertheless, the metabolite series expanded with time in plasma in a manner consistent with processive exonuclease-mediated degradation. A similar metabolite pattern was observed in tissues from 10 min onwards. Tissue concentrations increased in concert with the clearance of CGP 69846A and chain-shortened metabolites from plasma. Maximal organ concentrations of oligonucleotides were achieved between 120 and 360 min before gradually decreasing through to 1440 min. Clearly, intact CGP 69846A and its major metabolites had significant tissue half-lives *in vivo*. The concentration–time profiles for CGP 69846A and its major metabolites (i.e. N_{-1} to N_{-5}) differed in the kidney and liver over 1440 min. In the kidney, the profiles for the parent and major metabolites changed in parallel, whereas in the liver there was a progressive increase in the T_{max} across the series CGP 69846A, N_{-1}, N_{-2}, N_{-3}, N_{-4}, and N_{-5}. The most plausible explanation for this is that the liver is capable of metabolising phosphorothioate oligonucleotides, whereas the kidney does not cause significant biotransformation in rats over a 1440 min time course.

Agreement between the tissue concentrations of [^{3}H]CGP 69846A by radiochemical quantitation and the total oligonucleotide pool by capillary gel electrophoresis was achieved. These data show that extraction and capil-

TABLE 5. Rate and extent of absorption following subcutaneous administration of [^{3}H]CGP 69846A to rats

Dose (mg/kg)	AUC (µg · min/L)	C_{max} (µg equiv/ml)	T_{max} (min)	Bioavailabilitiy (%)	Recovery† (%)
0.6	109.0	0.37 ± 0.14	30	41	43
6.0	2508.6	12.80 ± 1.20	60	43	61
60.0	71820.0	154.16 ± 4.11	120	101	79

Bioavailability = $(AUC_{subcutaneous}/AUC_{intravenous})*100$, where AUCs are compared at equal doses.
† Recovery values do not include the site of administration.

TABLE 6. Capillary gel electrophoretic analysis of CGP 69846A and its metabolites in plasma, kidney, and liver following intravenous and subcutaneous administration to rats

	Percent of total									
	N	N_{-1}	N_{-2}	N_{-3}	N_{-4}	N_{-5}	N_{-6}	N_{-7}	N_{-8}	N_{-9}
Intravenous 360 min										
Kidney	21.1 ± 1.3	18.3 ± 1.2	16.4 ± 1.0	13.0 ± 0.5	8.3 ± 0.4	6.8 ± 0.5	6.1 ± 0.6	4.0 ± 0.6	4.2 ± 0.9	2.7 ± 0.9
Liver	38.1 ± 2.9	26.2 ± 1.6	14.8 ± 0.1	7.9 ± 1.5	3.4 ± 1.2	1.8 ± 0.6	2.5 ± 1.1	1.4 ± 0.3	0.1 ± 0.1	0.47
Intravenous 1440 min										
Kidney	27.2 ± 1.4	23.4 ± 1.1	18.6 ± 0.7	13.5 ± 0.1	6.5 ± 0.3	4.8 ± 0.8	3.1 ± 0.9	0.8 ± 0.4	0.7 ± 0.3	n.d.
Liver	23.6 ± 0.4	21.2 ± 0.6	14.3 ± 0.2	10.1 ± 0.3	9.4 ± 0.1	5.7 ± 1.3	5.0 ± 1.0	2.0 ± 0.6	n.d.	n.d.
Subcutaneous 360 min										
Kidney	16.1 ± 0.8	14.4 ± 0.4	14.0 ± 0.2	12.0 ± 0.2	9.4 ± 0.0	7.7 ± 0.4	7.4 ± 0.3	6.3 ± 0.4	6.3 ± 0.3	4.5 ± 0.3
Liver	30.5 ± 3.3	24.0 ± 2.0	16.5 ± 1.7	10.9 ± 0.5	7.5 ± 0.9	2.9 ± 1.6	2.2 ± 1.1	0.8 ± 0.6	n.d.	n.d.
Subcutaneous 1440 min										
Kidney	12.0 ± 0.7	12.4 ± 0.7	12.1 ± 0.4	11.1 ± 0.8	10.4 ± 0.2	8.9 ± 0.3	8.9 ± 0.4	8.3 ± 0.5	8.0 ± 1.0	5.2 ± 1.0
Liver	27.3 ± 3.1	23.2 ± 1.8	15.4 ± 0.5	10.7 ± 0.3	9.5 ± 1.2	6.4 ± 0.3	3.9 ± 0.1	1.5 ± 0.7	n.d.	n.d.

Data represent mean ± SEM for three animals, where metabolites are not present on all three animals mean values are given without experimental errors. n.d. = not detected.

lary gel electrophoresis methods have the required efficiency, resolution, sensitivity, and reproducibility to provide reasonably specific information about the concentration–time profiles for CGP 69846A and its metabolites. These data, together with other recent reports [15], support capillary electrophoresis becoming the minimum analytical method required to support oligonucleotide pharmacokinetic studies.

Metabolic chain-shortening of phosphorothioate oligonucleotides *in vivo* has been widely observed [8, 13–15] and attributed to 3′-exonuclease-mediated cleavage through indirect experimental evidence. Temsamani *et al.* [25] showed that 3′-capping, but not 5′-capping, of a phosphorothioate oligonucleotide increased its *in vivo* stability compared to the uncapped compound. Furthermore, phosphorothioate oligonucleotides self-stabilised with a 3′-hairpin loop were more stable *in vitro* [26] and *in vivo* [26, 27] compared with their linear counterparts. In the present study we have used electrospray mass spectrometry to define molecular weights for the metabolic products of CGP 69846A in rat liver extracts. By comparison with calculated molecular weights, metabolites having masses consistent with 3′-cleavage alone, 5′-cleavage alone and combined 3′- and 5′-cleavage were observed. These data from rat liver suggest that in addition to the assumed 3′-degradation, 5′-exonucleases are capable of degrading this phosphorothioate oligonucleotide. In addition, a series of more subtle metabolites (−16 Da) were observed, and one can speculate that these metabolites may arise through an exchange of sulphur with oxygen (i.e. metabolic oxidation) at a phosphorothioate linkage. In line wth the observations of Agrawal *et al.* [8], metabolites with a lower electrophoretic mobility than CGP 69846A (N_{+x}) were detected but not defined.

In agreement with previous results [11, 14], we have shown that a single intravenous dose of CGP 69846A was slowly excreted and significant levels of the parent compound and its metabolites remained in the tissues after 1440 min (1 day). By monitoring tissue radioactivity, Cossum *et*

FIG. 7. Wholebody autoradiography distribution and elimination studies in mice. A total [^{35}S]CGP 69846A dose of 1 μCi of was administered according to the dosage regimens described in Table 1. Groups 1 through 4 are shown sequentially from top to bottom. Representative autoradiograms are shown from $n = 4$.

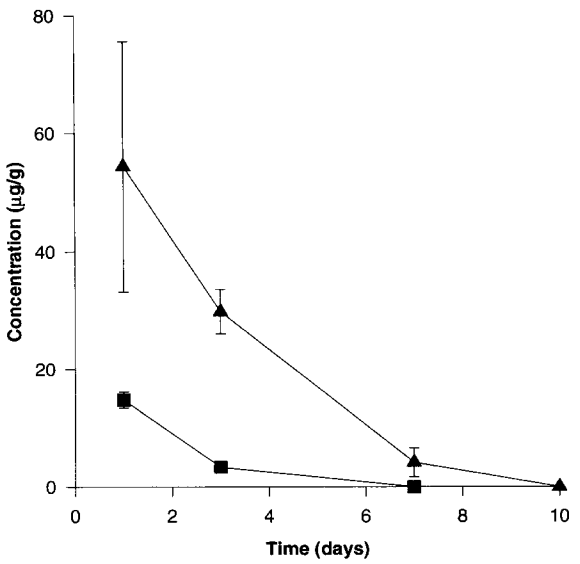

FIG. 8. Elimination of CGP 69846A from kidney and liver in mice. The elimination of CGP 69846A and derived metabolites from kidney (triangle) and liver (square) over time was determined using capillary gel electrophoresis. Mean ± SEM, $n = 3$.

al. [11] showed that a [^{14}C]-labelled 20-mer phosphorothioate oligonucleotide (ISIS 2105 at 3.6 mg/kg) was slowly cleared with low tissue levels persisting at 10 days. The clearance of a [^{35}S]-labelled 25-mer phosphorothioate oligonucleotide (GEM-91 at 30 mg/kg) appeared to occur more slowly, this being most notable from the kidney [14]. In the present study the clearance of CGP 69846A from organs over prolonged periods was investigated using whole-body autoradiography and analysis of tissue extracts by capillary gel electrophoresis. The combination of these methods enables a wide range of tissues to be monitored simultaneously and reasonably specific information about the clearance of CGP 69846A and its metabolites rather than relying on radiolabel alone. Tissue-associated radioactivity was much reduced after 7 days; low levels were still present in the kidney cortex and trace levels were associated with the liver. The whole-body clearance was reflected in the analysis of kidney and liver samples by capillary gel electrophoresis, which also show progressive metabolism of the CGP 69846A with time. CGP 69846A and its oligonucleotide metabolites were completely eliminated within 10 days following a single dose in the 6 to 10 mg/kg range. This rate of tissue clearance was similar to ISIS 2105 and greater than that for GEM-91. Further experiments are required to determine the reason for this difference. The rate of tissue clearance, for instance, may be dose dependent or related to the length of the parent compound and hence its major metabolites. Whole-body autoradiography studies also showed that the tissue distribution of CGP 69846A did not change upon repeated daily administration at 10 mg/kg for 7 days.

Additional studies have shown subcutaneous administration to be an efficient parenteral route, resulting in a rapid systemic delivery and a comparable tissue distribution to intravenous dosing. The blood profile was similar to that reported for another phosphorothioate oligonucleotide [13]; blood levels peaked rapidly, achieving concentrations approximately 4.5-fold lower than for the same dose given as an intravenous bolus, and then tailed off slowly. The absolute bioavailability and time to achieve maximum blood levels of CGP 69846A increased with dose. Saturation of local binding at the site of administration is the most attractive explanation of this dose dependence. Preclinical studies in monkeys, have shown that phosphorothioate oligonucleotides can elicit anticoagulation and complement activation when plasma concentrations exceed threshold levels [3, 28]. These haemodynamic side effects are dose rate limiting rather than dose limiting, because they can be avoided by slow intravenous infusion of the oligonucleotide instead of bolus administration [29]. Subcutaneous dosing, an alternative approach to reducing the rate of dose input, would be clinically attractive in terms of ease of administration and patient convenience. Despite slightly greater metabolism after subcutaneous dosing, our subcutaneous data are encouraging and suggest further studies in nonrodent species are warranted to explore the clinical potential of this administration route.

In summary, the disposition of a 20-mer phosphorothioate oligonucleotide has been described in detail. We have shown intravenously administered [^{3}H]CGP 69846A to be rapidly cleared from blood and distributed amongst high (e.g. kidney, liver, spleen), low (e.g. lung, skeletal muscle, skin), and negligible (e.g. brain, fat) accumulating tissues. Furthermore, its disposition was dose dependent. These radiochemical studies were supported by the analysis of tissue extracts using capillary gel electrophoresis. CGP 69846A was rapidly metabolised in plasma; parent compound represented 60.9, 48.3, and 18.1% of the total oligonucleotide pool at 10, 120, and 360 min with the remainder being chain-shortened metabolites (N_{-n}) having greater electrophoretic mobility. A similar metabolite profile was observed in kidney and liver. Extracts were further analysed by electrospray mass spectrometry—chain-shortened metabolites having a masses consistent with 3′-, 5′- and both 3′- and 5′-exonuclease-mediated degradation were present in the liver at 1440 min. The subcutaneous administration was also shown to be promising for CGP 69846A. It resulted in the rapid appearance of CGP 69846A in the systemic circulation, a similar distribution to high, low, and negligible accumulating tissues and only slightly greater oligonucleotide metabolism. Maximum blood concentrations were 4.5-fold lower than an equivalent dose given intravenously with low interanimal variability. The pharmacokinetic handling of oligonucleotides has received considerable attention and latterly with increasingly sophisticated analysis. Nevertheless, significant issues remain—(i) what is the influence of oligonucleotide sequence on pharmacokinetics?; (ii) what factors govern the pharmacokinetic properties of oligonucleotides e.g. protein binding, cellular recognition and uptake?; (iii) what is the cellular and subcellular distribution of oligonucleo-

tides *in vivo*?; (iv) how are oligonucleotides metabolised and eliminated?; (v) what is the effect of repeated administration on the disposition of oligonucleotides?; and (vi) can oligonucleotides achieve systemic availability following nonparenteral administration—and are currently under investigation in our laboratories for phosphorothioates and other chemical modifications.

The authors would like to thank Drs. Karl-Heinz Altmann, Aran Paulus, Len Cummins, Mark Graham, and Brett Monia for their support throughout this work. We thank Drs. John Hastewell, Gino van Heeke, Colin Howes, and Heinz Moser for their constructive criticism of the manuscript.

References

1. Zamecnik PC and Stevenson ML, Inhibition of Rouse sarcoma virus replication and cell transformation by a specific oligodeoxynucleotide. *Proc Natl Acad Sci USA* **75:** 280–284, 1978.
2. Helene C and Toulme JJ, Specific regulation of gene expression by antisense, sense and antigene nucleic acids. *Biochim Biophys Acta* **1049:** 99–125, 1990.
3. Crooke ST, Therapeutic applications of oligonucleotides. R. G. Landes Co., Austin, TX, 1995.
4. Higgins KA, Perez JR, Coleman TA, Dorshkind K, McComas WA, Sarmiento UM, Rosen CA and Narayanan R, Antisense inhibition of the p65 subunit of NF-κB blocks tumorigenicity and causes tumor regression. *Proc Natl Acad Sci USA* **90:** 9901–9905, 1993.
5. Monia BP, Johnston JF, Geiger T, Mueller M and Fabbro D, Antitumor activity of a phosphorothioate antisense oligodeoxynucleotide targeted against c-*raf* kinase. *Nat Med* **2:** 668–675, 1996.
6. Dean NM, McKay R, Miraglia L, Howard R, Cooper S, Giddings J, Nicklin PL, Miester L, Ziel R, Geiger T, Müller M and Fabbro D, Inhibition of human tumor cell lines in nude mice by an antisense inhibitor of PKC-α expression. *Cancer Res* **56:** 3499–3507, 1996.
7. Agrawal S, Antisense oligonucleotides as antiviral agents. *Trends Biotechnol Sci* **10:** 152–157, 1992.
8. Agrawal S, Temsamani J and Tang JY, Pharmacokinetics, biodistribution and stability of oligodeoxynucleotide phosphorothioates in mice. *Proc Natl Acad Sci USA* **88:** 7595–7599, 1991.
9. Goodarzi G, Watabe M and Watabe K, Organ distribution and stability of phosphorothioated oligodeoxyribonucleotides in mice. *Biopharmacol Drug Dispos* **13:** 221–227, 1992.
10. Iversen P, *In vivo* studies with phosphorothioate oligonucleotides: Pharmacokinetics prologue. *AntiCancer Drug Design* **6:** 531–538, 1991.
11. Cossum PA, Sasmor H, Dellinger D, Truong L, Cummins L, Owens SR, Markham PM, Shea JP and Crooke ST, Disposition of the ^{14}C-labeled phosphorothioate oligonucleotide ISIS 2105 after intravenous administration to rats. *J Pharmacol Exp Ther* **267:** 1181–1190, 1993.
12. Sands H, Gorey-Feret LJ, Cocuzza AJ, Hobbs FW, Chidester D and Trainor GL, Biodistribution and metabolism of internally ^{3}H-labeled oligonucleotides. 1. Comparison of a phosphodiester and a phosphorothioate. *Mol Pharmacol* **45:** 932–943, 1994.
13. Agrawal S, Temsamani J, Galbraith W and Tang J, Pharmacokinetics of antisense oligonucleotides. *Clin Pharmacokinet* **28:** 7–16, 1995.
14. Zhang R, Diasio RB, Lu Z, Liu T, Jiang Z, Galbraith WM and Agrawal S, Pharmacokinetics and tissue distribution in rats of an oligodeoxynucleotide phosphorothioate (GEM-91) developed as a therapeutic agent for human immunodeficiency virus type-1. *Biochem Pharmacol* **49:** 929–939, 1995.
15. Crooke ST, Graham MJ, Zuckerman JE, Brooks D, Conklin BS, Cummins LL, Greig MJ, Kornburst D, Manoharan M, Sasmor H, Schleich T, Tivel KL and Griffey R, Pharmacokinetic properties of several oligonucleotide analogs in mice. *J Pharmacol Exp Ther* **277:** 923–937, 1996.
16. Rifai A, Brysch W, Fadden K, Clark J and Schlingensiepen K-H, Clearance kinetics, biodistribution and organ saturability of phosphorothioate oligodeoxynucleotides in mice. *Am J Pathol* **149:** 717–725, 1996.
17. Cossum PA, Sasmor H, Dellinger D, Truong L, Cummins L, Owens SR, Markham PM, Shea JP and Crooke ST, Disposition of the ^{14}C-labeled phosphorothioate oligonucleotide ISIS 2105 after intradermal administration to rats. *J Pharmacol Exp Ther* **269:** 89–94, 1994.
18. Saijo Y, Perlaky L, Wang H and Busch H, Pharmacokinetics, tissue distribution and stability of antisense oligodeoxynucleotide phosophorothioate ISIS 3466 in mice. *Oncol Res* **6:** 243–249, 1994.
19. Leeds JM, Graham MJ, Truong L and Cummins LL, Quantification of phosphorothioate oligonucleotides in human plasma. *Anal Biochem* **235:** 36–43, 1996.
20. Graham MJ, Freier SM, Crooke RM, Ecker DJ, Maslova RN and Lesnik EA, Tritium labeling of antisense oligonucleotides by exchange with tritiated water. *Nucleic Acids Res* **21:** 3737–3743, 1993.
21. Williamson I, Phillips JA and Nicklin PL, Pharmacokinetics, organ distribution and cellular uptake of phosphorothioate oligonucleotides *in vivo*. Proceedings of the International Conference 'Therapeutic oligonucleotides from Cell to Man', 1995.
22. Crooke RM, *In vitro* toxicology and pharmacokinetics of antisense oligonucleotides. *Anticancer Drug Design* **6:** 609–646, 1991.
23. Beck GF, Irwin WJ, Nicklin PL and Akhtar S, Interactions of phosphodiester and phosphorothioate oligonucleotides with intestinal epithelial cells. *Pharmacol Res* **13:** 1028–1037, 1996.
24. Spitzer S and Eckstein F, Inhibition of deoxyribonucleases by phosphorothioate groups in oligodeoxyribonucleotides. *Nucleic Acids Res* **16:** 11691–11704, 1988.
25. Temsamani J, Tang JY, Padmapriya A, Kubert M and Agrawal S, Pharmacokinetics, biodistribution and stability of capped oligodeoxynucleotide phosphorothioates in mice. *Antisense Res Dev* **3:** 277–284, 1993.
26. Tang JY, Temsamani J and Agrawal S, Self-stabilized antisense oligodeoxynucleotide phosphorothioates: Properties and anti-HIV activity. *Nucleic Acids Res* **21:** 2729–2735, 1993.
27. Zhang R, Lu Z, Zhang X, Zhao H, Diasio RB, Liu T, Jiang Z and Agrawal S, *In vivo* stability and disposition of a self-stabilized oligodeoxynucleotide phosphorothioate in rats. *Clin Chem* **41:** 836–843, 1995.
28. Galbraith WM, Hobson WC, Giclas PC, Schechter PJ and Agrawal S, Complement activation and hemodynamic changes following intravenous administration of phosphorothioate oligonucleotides in the monkey. *Antisense Res Dev* **4:** 201–206, 1994.
29. Cornish KG, Iversen P, Smith L, Arneson M and Bayever E, Cardiovascular effects of a phosphorothioate oligonucleotide with a sequence antisense to p53 in the conscious rhesus monkey. *Pharmacol Commun* **3:** 239–247, 1993.